BHR Group
EXPERTS IN FLUID ENGINEERING

Explanation for the frequency shift pattern of non-uniform blocked pipeline systems from an energy perspective

T.C. Che[1], H.F. Duan[1], B. Pan[1], P.J. Lee[2] & M.S. Ghidaoui[3]

[1]*Department of Civil and Environmental Engineering, The Hong Kong Polytechnic University, Hong Kong SAR, PR China.*
[2]*Department of Civil and Natural Resources Engineering, The University of Canterbury, New Zealand.*
[3]*Department of Civil and Environmental Engineering, The Hong Kong University of Science and Technology, Hong Kong SAR, PR China.*

ABSTRACT
It was found in a previous study that the transient frequency shifts induced by non-uniform blockages in water pipelines become less evident as the frequency increases, but its physical mechanism is unclear. This paper explains this non-uniform blockage induced frequency shift pattern from an energy perspective. The results indicate that the non-uniform blockages have a less blocking effect on the propagation of high frequency waves; thus, the induced frequency shifts become less evident. In practical applications of non-uniform blockage detection, the frequency of the incident wave should be selected carefully to ensure that the reflected wave contains enough energy.

Keywords: Energy transmission coefficient; frequency shift; non-uniform blockage; transfer matrix; transient; water pipeline

1 INTRODUCTION

Extended partial blockages in urban water supply systems (UWSS), which are formed from various complicated sources (e.g., chemical corrosion, biofilm accumulation, and sediment deposition), present a major challenge for drinking water security as well as water and energy savings. Detection techniques are in urgent need to inspect these blockages at the early stage so as to minimize the caused problems and wastage. Currently, internal inspection of pipelines by CCTV cameras is a commonly used approach for practical extended blockage detection (1). These CCTV cameras are fed into the target pipelines to conduct a real-time internal inspection of the pipe wall condition. But this technique is more suitable for simple and small-scale pipeline systems (e.g., pipeline systems in thermal power plants) since inspection by CCTV cameras is a slow, tedious, and costly process. In addition, it needs off-line and destructive operations on target pipelines, and the service interruption might cause inconvenience to users. Therefore, it is vital to develop an efficient, affordable, and non-destructive method for extended blockage detection.

Transient pressure waves, with propagation speeds up to 1 km/s in elastic water pipelines, have been used for the detection of many pipeline faults including leaks (2-6), discrete blockages (7-10), and dead ends (11). A transient wave is injected into the UWSS at a localized accessible point (e.g., a fire hydrant). The injected wave is modified by any pipeline faults as it propagates in the pipeline; thus, the measured modified wave in theory contains useful physical information for pipeline fault and system integrity identification. In recent years, the successful theoretical and experimental extensions of the transient-based method to extended blockage detection provide an alternative to the CCTV cameras. Specifically, it was found that extended blockages induce frequency shifts on the resonant peaks of pipeline systems (12), based on which Duan, et al. (12) proposed an optimization method for the inverse detection of extended blockages in pressurized pipelines. This proposed method was further verified by a series of laboratory experiments (13). Afterwards, Louati, et al. (14) explained the physical mechanism of the blockage induced frequency shifts by the Bragg resonance theory.

Although the transient-based method has been demonstrated its potential for extended blockage detection, this method is developed based on blockages in the uniform shape. In the real UWSS, partial and extended blockages are formed from a series of complicated physical, chemical, and biological processes; thus, as shown in Figure 1(a), they are generally in random and non-uniform shapes. Inaccuracy and invalidity of the current transient-based method have been observed in laboratories for non-uniform blockage detection (15). To enhance the practical application of the current transient-based method, it is necessary to further investigate the interaction between transient waves and non-uniform blockages.

Recently, the authors analysed the influence of non-uniform blockages, with linearly varying diameters (termed as linear non-uniform blockage), on transient frequency responses (16). It shows that linear non-uniform blockages induce different resonant frequency shift patterns from uniform blockages. Specifically, the frequency shifts induced by linear non-uniform blockages become less evident with the increase of frequency (termed as non-uniform blockage induced frequency shift pattern), but the physical mechanism of this non-uniform blockage induced frequency shift pattern from the theoretical and numerical results is still not well understood.

This paper intends to (1) further investigate the frequency shift pattern induced by other non-uniform blockages with non-linearly (i.e., exponentially) varying diameters to generalize the conclusions drawn in the previous study on linear non-uniform blockages (16); and (2) qualitatively explain the physical mechanism of the non-uniform blockage induced frequency shift pattern from an energy perspective. In particular, the overall transfer matrices of pipeline systems with exponential non-uniform blockages are derived to realize the Aim (1). To achieve the Aim (2), the energy transmission coefficients (TC) of pipe flow systems with blockages are analytically derived based on the system overall transfer matrices. The results and findings of this study are expected to provide scientific basis for the method development of extended blockage detection in the real UWSS.

2 MODELS AND METHODS

2.1 Overall transfer matrix of a non-uniform blocked pipeline system

The one-dimensional (1D) wave equation for the *n*-th exponential non-uniform blockage, as shown in Figure 1(b), in the frequency domain is (16)

$$\frac{\mathrm{d}^2 p_n}{\mathrm{d}x^2} + \frac{1}{A_n}\frac{\mathrm{d}A_n}{\mathrm{d}x}\frac{\mathrm{d}p_n}{\mathrm{d}x} + k_0^2 p_n = 0 \tag{1}$$

where p = pressure deviation in the frequency domain; x = distance along the pipeline; A = $A(x)$ = pipe cross-sectional area; k_0 = ω/a_0 = wave number, in which ω = angular frequency, a_0 = wave speed, which is assumed to be constant throughout the pipeline system to simplify the problem; subscript n = the n-th exponential non-uniform blockage.

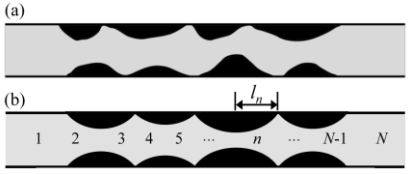

Figure 1. (a) Sketch of a realistic pipeline with non-uniform blockages; (b) sketch of a pipeline with exponential non-uniform blockages used for analytical analysis

The pipe radius of the n-th exponential blockage can be expressed as

$$r_n(x) = R_{Ln} e^{s_n x} \tag{2}$$

where r_n = pipe radius of the n-th exponential non-uniform blockage; R_{Ln} = pipe radius at the left boundary of the n-th exponential non-uniform blockage; s_n = a coefficient that determines the radius changing rate of n-th exponential non-uniform blockage.

The general solutions of the wave equation for the n-th exponential non-uniform blockage are plane wave solutions (17)

$$(p_n)_1 = \frac{e^{ik'x}}{R_{Ln}e^{s_n x}},\ (p_n)_2 = \frac{e^{-ik'x}}{R_{Ln}e^{s_n x}} \tag{3}$$

where $k' = (k_0^2 - s_n^2)^{1/2}$.

Based on the general solutions in Eq. (3), the transfer matrix of the n-th exponential non-uniform blockage connecting two state vectors at two boundaries is (16, 17) (note that the pressure deviation p is transformed into the pressure head deviation h)

$$\begin{pmatrix} q \\ h \end{pmatrix}_{n+1} = \begin{pmatrix} U_{11} & U_{12} \\ U_{21} & U_{22} \end{pmatrix} \begin{pmatrix} q \\ h \end{pmatrix}_n \tag{4}$$

where q = discharge deviation in the frequency domain; h = pressure head deviation in the frequency domain; U_{ij} = transfer matrix elements, which are in the following forms

$$U_{11} = \frac{A_{n+1}}{A_n}\frac{\left(ik' - s_n\right)e^{ik'l_n} + \left(ik' + s_n\right)e^{-ik'l_n}}{2ik'e^{s_n l_n}}$$

$$U_{12} = \frac{A_{n+1}g\left(ik' - s_n\right)\left(ik' + s_n\right)}{\omega}\frac{e^{ik'l_n} - e^{-ik'l_n}}{2k'e^{s_n l_n}}$$

$$U_{21} = \frac{\omega}{A_n g} \frac{-e^{ik' l_n} + e^{-ik' l_n}}{2k' e^{s_n l_n}}$$

$$U_{22} = \frac{\left(ik' + s_n\right) e^{ik' l_n} + \left(ik' - s_n\right) e^{-ik' l_n}}{2ik' e^{s_n l_n}}$$

Note that the uniform blockage is one special case of the exponential non-uniform blockage. Let $s_n = 0$, which is equivalent to a single uniform pipeline, Eq. (4) becomes

$$\begin{pmatrix} q \\ h \end{pmatrix}_{n+1} = \begin{pmatrix} \cos\left(k_0 l_n\right) & -i \frac{A_{n+1} g}{a} \sin\left(k_0 l_n\right) \\ -i \frac{a}{A_n g} \sin\left(k_0 l_n\right) & \cos\left(k_0 l_n\right) \end{pmatrix} \begin{pmatrix} q \\ h \end{pmatrix}_n \tag{5}$$

which is consistent with previous studies on uniform pipelines (18).

The overall transfer matrix of a blocked pipeline system, as shown in Figure 1(b), can be produced by multiplying individual matrices of each pipe component in the order of their locations (3).

$$\begin{pmatrix} q \\ h \end{pmatrix}_{\text{down}} = \begin{pmatrix} U_{11}^* & U_{12}^* \\ U_{21}^* & U_{22}^* \end{pmatrix} \begin{pmatrix} q \\ h \end{pmatrix}_{\text{up}} \tag{6}$$

where U_{ij}^* = elements of the overall transfer matrix; subscripts "down" and "up" are locations of upstream and downstream boundaries of a blocked pipeline system, as shown in Figure 1(b), respectively.

2.2 Energy transmission coefficient of an unbounded blocked pipeline system

Based on the above overall transfer matrix (i.e., Eq. (6)), the energy transmission coefficient (TC) of an unbounded blocked pipeline system is derived in this section. To simplify the problem, a pipeline system with two symmetrical exponential non-uniform blockages, as shown in Figure 2, is selected for investigation. Note that the derived TC can be also applied to pipeline systems with multiple non-uniform blockages (see Figure 1(b)) as long as the system overall transfer matrix is determined.

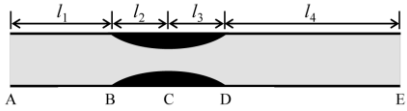

Figure 2. A pipeline system with two exponential non-uniform blockages

In physics, a transient wave is a pressure disturbance that travels through fluids, accompanied by a transfer of energy. The energy flow (i.e., power) passing through a unit cross-sectional area of a pipe (termed as power intensity) is defined as (19)

$$I = \frac{1}{T} \int_0^T p^* u^* dt \tag{7}$$

where I = power intensity; $T = 2\pi/\omega$ for time-harmonic waves; p^* = pressure deviation from the mean in the time domain; u^* = axial velocity deviation from the mean in the time domain (at upstream and downstream boundaries).

In classical acoustics, including water hammer problems focused on herein, it is often assumed that p^* and u^* are time-harmonic waves (16, 18)

$$p^* = pe^{i\omega t},\ u^* = ue^{i\omega t} \tag{8}$$

where p and u are complex amplitudes; i = imaginary number. Specifically, let $u = |u|e^{i\theta}$, where $|u|$ = amplitude; θ = initial phase.

In the transient pipe flow analysis, the impedance is usually used for describing the transient wave propagation characteristics of specified pipelines, which is defined as

$$Z = \frac{p^*}{u^*} = \frac{p}{u} = \mathrm{Re}(Z) + i\,\mathrm{Im}(Z) = |Z|e^{i\phi} \tag{9}$$

where Z = impedance; Re() = real part; Im() = imaginary part; Re(Z) = resistance; Im(Z) = reactance; ϕ = phase angle between p^* and u^*.

Substituting Eq. (9) into Eq. (7), it becomes

$$\begin{aligned} I &= \frac{\omega}{2\pi}\int_0^{2\pi/\omega} \mathrm{Re}\left(Zu^*\right)\mathrm{Re}\left(u^*\right)dt \\ &= \frac{\omega}{2\pi}\int_0^{2\pi/\omega} |Z||u|^2 \cos\left(\omega t+\theta+\phi\right)\cos\left(\omega t+\theta\right)dt \\ &= \frac{1}{2}|u|^2|Z|\cos\phi \\ &= \frac{1}{2}|u|^2\,\mathrm{Re}(Z) \end{aligned} \tag{10}$$

As shown in Figure 2, for the upstream (i.e., location A) and downstream (i.e., location E) boundaries with a cross-sectional area A, the energy flow passing through this area is

$$W = IA = \frac{1}{2}|u|^2\,\mathrm{Re}(Z)A \tag{11}$$

The TC of a blocked pipeline system with anechoic boundaries (i.e., located at A and E), as shown in Figure 2, is defined as the ratio between the energy flow incident on the non-uniform blockages (W_{in}) and that transmitted through the non-uniform blockages (W_{tr}).

$$TC = \frac{W_{tr}}{W_{in}} \tag{12}$$

where TC = energy transmission coefficient.

The general solutions for p of the 1D wave equation in intact Pipe 1 and Pipe 4, as shown in Figure 2, are (20)

$$p = Me^{-ik_0 x} + Ne^{ik_0 x} \tag{13}$$

where M and N are wave amplitudes.

Substituting Eq. (13) into the frictionless 1D water hammer model, the following general solutions for u can be obtained

$$u = \frac{1}{\rho_0 a_0}\left(Me^{-ik_0 x} - Ne^{ik_0 x}\right) \tag{14}$$

where ρ_0 = fluid density.

The energy flow generated at the downstream boundary (i.e., located at E) is

$$W_{in} = \frac{1}{2\rho_0 a_0}\left|M_{\mathrm{E}}\right|^2 \mathrm{Re}(Z)\,A = \frac{\left|M_{\mathrm{E}}\right|^2}{2}A \tag{15}$$

Similarly, the energy flow transmitted through the non-uniform blockages is

$$W_{tr} = \frac{1}{2\rho_0 a_0}\left|M_{\mathrm{A}}\right|^2 \mathrm{Re}(Z)\,A = \frac{\left|M_{\mathrm{A}}\right|^2}{2}A \tag{16}$$

Therefore, the TC of the unbounded blocked pipeline system in Figure 2 is

$$TC = \frac{W_{tr}}{W_{in}} = \left|\frac{M_{\mathrm{A}}}{M_{\mathrm{E}}}\right|^2 \tag{17}$$

The amplitude of a progressive wave keeps constant as it travels along a uniform pipe (21). As shown in Figure 2, M_{A} and M_{E} can be measured at any point along Pipe 1 and Pipe 4, respectively. To simplify the mathematical calculation, lengths l_1 and l_4 can be taken as zero if necessary.

The overall transfer matrix (in terms of u and p) of a blocked pipeline system, as shown in Figure 2, is

$$\begin{Bmatrix} u \\ p \end{Bmatrix}_{\mathrm{E}} = \begin{bmatrix} V_{11}^* & V_{12}^* \\ V_{21}^* & V_{22}^* \end{bmatrix} \begin{Bmatrix} u \\ p \end{Bmatrix}_{\mathrm{A}} \tag{18}$$

where V_{ij}^* = elements of the overall transfer matrix (in terms of u and p).

Based on the general solutions in Eqs. (13) and (14), the p and u at two locations A and D can be expressed as (note that $N_{\mathrm{A}} = 0$)

$$p_{\mathrm{A}} = M_{\mathrm{A}} + N_{\mathrm{A}} = M_{\mathrm{A}} \tag{19a}$$

$$u_{\mathrm{A}} = \frac{1}{\rho_0 a_0}\left(M_{\mathrm{A}} - N_{\mathrm{A}}\right) = \frac{M_{\mathrm{A}}}{\rho_0 a_0} \tag{19b}$$

$$p_{\mathrm{D}} = M_{\mathrm{E}} + N_{\mathrm{E}} \tag{19c}$$

$$u_{\mathrm{D}} = \frac{1}{\rho_0 a_0}\left(M_{\mathrm{E}} - N_{\mathrm{E}}\right) \tag{19d}$$

From Eqs. (19a) to (19d)

$$\begin{aligned} M_{\mathrm{E}} &= \frac{p_{\mathrm{D}} + \rho_0 a_0 u_{\mathrm{D}}}{2} = \frac{\left(V_{21}^* u_{\mathrm{A}} + V_{22}^* p_{\mathrm{A}}\right) + \rho_0 a_0 \left(V_{11}^* u_{\mathrm{A}} + V_{12}^* p_{\mathrm{A}}\right)}{2} \\ &= \frac{\left(V_{21}^* \dfrac{M_{\mathrm{A}}}{\rho_0 a_0} + V_{22}^* M_{\mathrm{A}}\right) + \rho_0 a_0 \left(V_{11}^* \dfrac{M_{\mathrm{A}}}{\rho_0 a_0} + V_{12}^* M_{\mathrm{A}}\right)}{2} \end{aligned} \tag{20}$$

The ratio between M_{A} and M_{E} is

$$\frac{M_{\mathrm{A}}}{M_{\mathrm{E}}} = \frac{2}{\dfrac{V_{21}^*}{\rho_0 a_0} + V_{22}^* + V_{11}^* + \rho_0 a_0 V_{12}^*} \tag{21}$$

Therefore, the TC is (in terms of u and p)

$$TC = \left|\frac{M_{\mathrm{A}}}{M_{\mathrm{E}}}\right|^2 = \left|\frac{2}{\dfrac{V_{21}^*}{\rho_0 a_0} + V_{22}^* + V_{11}^* + \rho_0 a_0 V_{12}^*}\right|^2 \tag{22}$$

In terms of discharge q and pressure head h, the overall transfer matrix of the unbounded pipeline system in Figure 2 is

$$\begin{Bmatrix} q \\ h \end{Bmatrix}_{\mathrm{E}} = \begin{bmatrix} U_{11}^* & U_{12}^* \\ U_{21}^* & U_{22}^* \end{bmatrix} \begin{Bmatrix} q \\ h \end{Bmatrix}_{\mathrm{A}} \tag{23}$$

Writing Eq. (23) in the equation form

$$A_{\mathrm{D}} u_{\mathrm{D}} = U_{11}^* A_{\mathrm{A}} u_{\mathrm{A}} + U_{12}^* \frac{p_{\mathrm{A}}}{\rho_0 g} \tag{24a}$$

$$\frac{p_{\mathrm{D}}}{\rho_0 g} = U_{21}^* A_{\mathrm{A}} u_{\mathrm{A}} + U_{22}^* \frac{p_{\mathrm{A}}}{\rho_0 g} \tag{24b}$$

Rewrite Eqs. (24) as

$$u_{\mathrm{D}} = \underbrace{\frac{A_{\mathrm{A}}}{A_{\mathrm{D}}} U_{11}^*}_{V_{11}^*} u_{\mathrm{A}} + \underbrace{\frac{U_{12}^*}{\rho_0 g A_{\mathrm{D}}}}_{V_{12}^*} p_{\mathrm{A}} \tag{25a}$$

$$p_{\mathrm{D}} = \underbrace{\rho_0 g A_{\mathrm{A}} U_{21}^*}_{V_{21}^*} u_{\mathrm{A}} + \underbrace{U_{22}^*}_{V_{22}^*} p_{\mathrm{A}} \tag{25b}$$

in which $A_A = A_D = A$.

Therefore, the TC is (in terms of q and h)

$$TC = \left| \frac{2}{\frac{gAU_{21}^*}{a_0} + U_{22}^* + U_{11}^* + \frac{a_0 U_{12}^*}{gA}} \right|^2 \tag{26}$$

2.3 Bragg resonance condition of unbounded blocked pipeline systems

Because the following results involve the Bragg resonance theory, there is a need to review related fundamental theory herein. Louati, et al. (14) studied the Bragg resonance phenomena in pressurized water pipelines with uniform blockages. As shown in Figure 3(a), an incident wave with a certain wave length (λ) originating from the right boundary (i.e., location E) impinges on the uniform blockage. From Location E to Location A, this incident wave first encounters a sudden constriction at Junction D, and then a sudden expansion at Junction B. Based on the Joukowsky's equation (22), the reflected wave from Junction D keeps the same sign with the incident wave. On the contrary, Junction B changes the sign of the reflected wave. In addition, the wave reflected by Junction B travels $2(l_2 + l_3)$ more than the reflected wave from Junction D. If $n\lambda = 2(l_2 + l_3)$, where n = 1, 2, 3…, the reflected waves from Junctions B and D experience destructive interference at Junction D, therefore the incident wave has the maximum transmission. If $(2n + 1)\lambda/2 = 2(l_2 + l_3)$, these two reflected waves experience constructive interference, then the incident wave has the maximum reflection.

But for the non-uniform blockages, as shown in Figures 3(b) and 3(c), the situation is different. The incident wave encounters a continuous constriction between Junctions C and D and a continuous expansion between Junctions B and C. The reflected wave from Junction C propagates $2l_3$ more than that from Junction D. Therefore, these two reflected waves experience destructive interference when $n\lambda = 2l_3$ and constructive interference when $(2n + 1)\lambda/2 = 2l_3$.

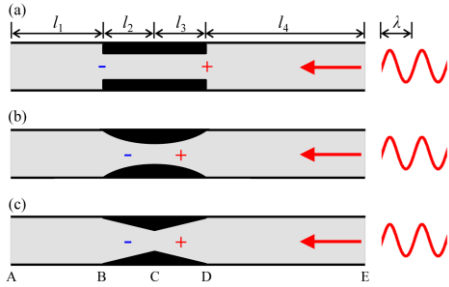

Figure 3. Pipeline systems with uniform and non-uniform blockages

Based on the derived TC in Eq. (26), the TC curves of pipeline systems containing both uniform and non-uniform (linear and exponential) blockages, with the same blocked volume, are plotted in Figure 4. For the convenience of comparison, the TC curve of an intact pipeline system (i.e., blockage-free case) is also plotted. The detailed parameters for these 4 cases are listed in Table 1, in which R = radius of the intact pipeline; R_C = pipe radius at the location C in Figure 3.

Table 1. Detailed pipeline system parameters for transmission coefficient calculations

Blockage type	l_1 (m)	l_2 (m)	l_3 (m)	l_4 (m)	R (m)	R_C (m)	$\|s\|$
blockage-free	300	100	100	500	0.25	0.25	0
uniform	300	100	100	500	0.25	0.20	0
non-uniform (linear)	300	100	100	500	0.25	0.15	1.00E-3
non-uniform (exp)	300	100	100	500	0.25	0.1572	4.64E-3

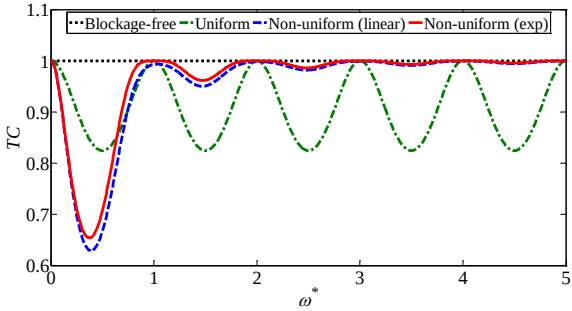

Figure 4. Transmission coefficients of intact and blocked pipeline systems

In Figure 4, the incident wave frequency is normalized by the minimum destructive frequency of the blockages, which is $2\pi(a_0/(2(l_2 + l_3)))$ for uniform blockages and $2\pi(a_0/(2l_3))$ for non-uniform blockages, and is expressed as ω^* in the x-axis. As shown in Figure 4, the TC of the intact pipeline system is frequency independent (i.e., keeps the constant value of 1), which is physically reasonable since no wave is reflected in an intact pipeline. However, the TC curves of three blocked pipeline systems are highly frequency dependent. Specifically, the TC curve of the uniform blocked pipeline varies periodically as the incident wave frequency increases. This is consistent with previous studies on uniform blockages (14, 20). Similarly, the TC curves of the two non-uniform blocked pipelines fluctuate periodically. Moreover, their amplitude periodically increases as the increase of the incident wave frequency. This means that the higher the incident wave frequency, the more energy is transmitted through the non-uniform blockages.

3 NUMERICAL VALIDATION

To numerically validate the derived analytical TC in Eq. (26), the frictionless 1D water hammer model coupling with the method of characteristics (MOC) is adopted in this section. Note that the upstream and downstream boundaries are anechoic. As shown in Figure 5, a wave generator and a wave receiver are located at the downstream and upstream of the blocked pipeline system, respectively. The incident wave generated at the generator is given by the following formula (i.e., a Gaussian-modulated sinusoidal pulse) (14)

$$P_{in} = P_0 + P_0 \exp\left(-4\left(\frac{\omega_c}{\beta}\right)^2 \log(10)\left(t - \left(\frac{\beta}{\omega_c}\right)^2\right)\right)\sin\left(\omega_c\left(t - \frac{\beta}{\omega_c}\right)\right) \tag{27}$$

where P_{in} = the incident wave pressure at the generator; P_0 = the initial pressure in the pipeline; ω_c = the angular central frequency of the incident wave; β = a coefficient that determines the frequency bandwidth of the incident wave; $0 < t \leq \beta/\omega_c$.

Most of energy of a Gaussian-modulated sinusoidal pulse is distributed at its central frequency ω_c, and the bandwidth of this pulse can be determined by appropriately adjusting the value of β.

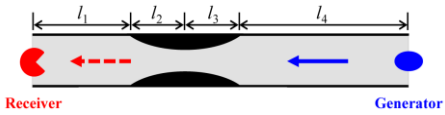

Figure 5. An unbounded blocked pipeline system with a wave generator and a wave receiver

The incident and transmitted waves measured at the generator and receiver are plotted in Figure 6(a). The pressure P is normalized according to $P^* = (P - P_0)/P_0$ and plotted as the y-axis. Figure 6(a) shows that the amplitude of the transmitted wave almost stays the same with that of the incident wave. To explain this, these time domain signals are further transformed into the frequency domain as shown in Figure 6(b). According to Figure 6(b), the central frequency of the incident wave is $\omega_c^* = 1$, at which the TC has a local maximum value 1.00, as shown in Figure 4, because of the destructive interference happened at the Junction D.

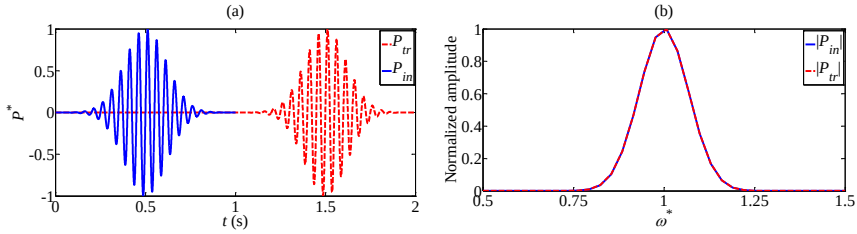

Figure 6. (a) Measured pressure signals in the time domain ($\omega_c^* = 1$); (b) corresponding pressure signals in the frequency domain ($\omega_c^* = 1$)

Similarly, three more points on the TC curve with local minimum values (i.e., at ω_c^* = 0.5, 1.5, and 2.5) are further examined. It can be observed from Figures 7(a), 7(c), and 7(e) that the amplitude of transmitted wave gradually increases as the increase of the incident wave frequency. This means that the higher the incident wave frequency, the more energy is transmitted through the non-uniform blockages. Based on Eq. (17) and the normalized frequency domain amplitude of transmitted waves in Figures 7(b), 7(d), and 7(f), the TC of these three points can be calculated as 0.71, 0.96, and 0.99, respectively, which agree well with the analytical values 0.71, 0.96, and 0.99 in Figure 4.

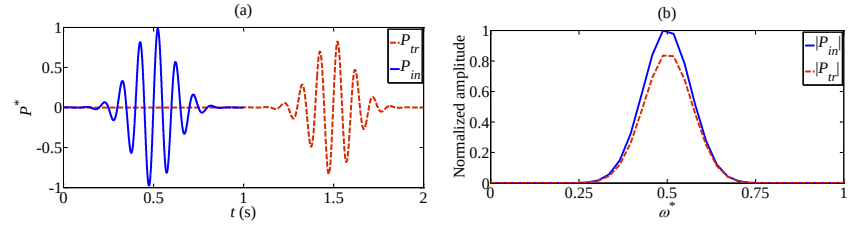

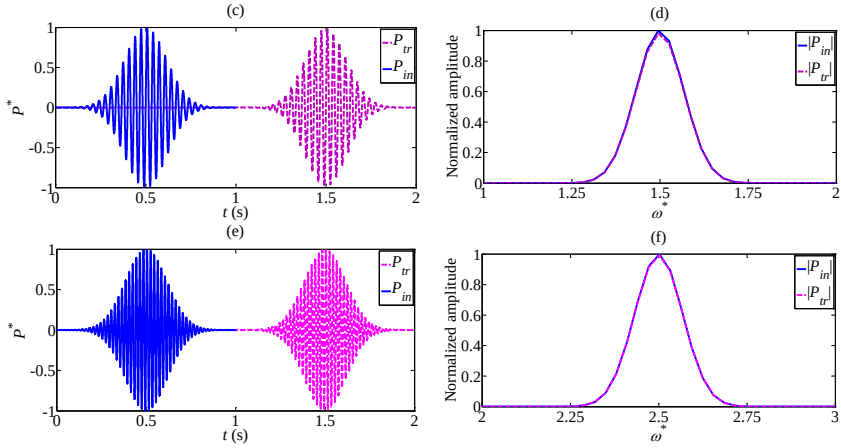

Figure 7. Measured pressure signals in the time domain (a) $\omega_c^* = 0.5$, (c) $\omega_c^* = 1.5$, (e) $\omega_c^* = 2.5$; (b) corresponding pressure signals in the frequency domain (b) $\omega_c^* = 0.5$, (d) $\omega_c^* = 1.5$, (f) $\omega_c^* = 2.5$

In addition, more points are numerically validated and plotted in Figure 8, it indicates good agreement between the numerical results and the analytical results. These numerical results confirm the validity of the derived TC as well as the analytical method adopted in this study.

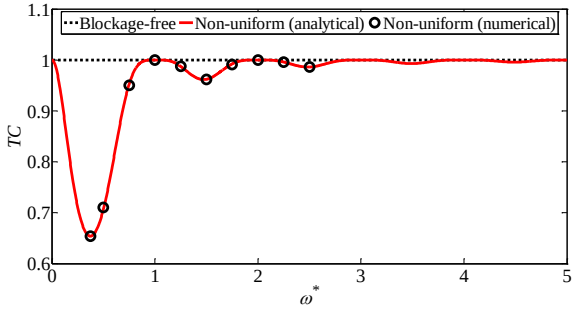

Figure 8. Numerical validation of TC

4 ENERGY EXPLANATION OF THE FREQUENCY SHIFT PATTERN

To further investigate and quantify the influence of non-uniform blockage properties (i.e., length, severity) on the TC of unbounded pipeline systems, five tests, as shown in Table 2, are conducted in this section for a systematic analysis. At the same time, the frequency shift patterns of bounded pipeline systems, as shown in Figure 9, with the same system parameters (i.e., Table 2) as the unbounded pipeline systems, are also obtained.

As shown in Table 2, the blockage lengths (i.e., l_2 and l_3) of Tests T1, T2, and T3 are fixed. From Test T1 to Test T3, the minimum radius R_C gradually increases from 0.15 m to 0.20 m, which means the blockage becomes less severe. The TC curves of these three tests are plotted in Figure 10(a). It shows that the overall trend of these TC curves is similar except for the amount of transmitted energy at a specific frequency. Specifically,

for a fixed incident wave frequency, more energy is transmitted through the non-uniform blockages as the blockages become less severe. This is physically reasonable since less severe blockages should have a less blocking effect on the transient wave propagation.

Table 2. Detailed pipeline system parameters of bounded and unbounded pipeline systems

Test no.	l_1 (m)	l_2 (m)	l_3 (m)	l_4 (m)	R (m)	R_C (m)	|s|
T1	300	100	100	500	0.25	0.15	5.11E-3
T2	300	100	100	500	0.25	0.175	3.57E-3
T3	300	100	100	500	0.25	0.20	2.23E-3
T4	390	10	10	590	0.25	0.15	5.11E-2
T5	399	1	1	599	0.25	0.15	5.11E-1

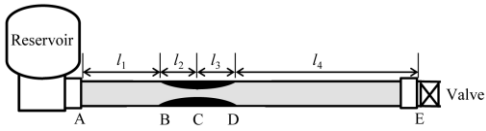

Figure 9. A bounded reservoir-pipeline-valve system

The frequency shift pattern of a bounded system (see Figure 9), with the same system parameters as Tests T1, T2, and T3, adopted from a previous study of the authors (16) are plotted in Figure 10(b). The frequency shift is defined as $\delta\omega^* = \omega_b^* - \omega_{in}^*$, in which ω_{in}^* = normalized resonance frequency of the intact pipeline system; ω_b^* = normalized resonance frequency of the blocked pipeline system. It is clearly shown that the frequency shift fluctuation induced by non-uniform blockages becomes less evident as the incident wave frequency increases. A possible explanation for this is that higher frequency incident waves, as shown in Figure 10(a), have higher TC (e.g., more than 0.96 when $\omega^* > 1$). This means non-uniform blockages have a less blocking effect on high frequency incident waves, thus the non-uniform blockage induced frequency shift becomes less evident.

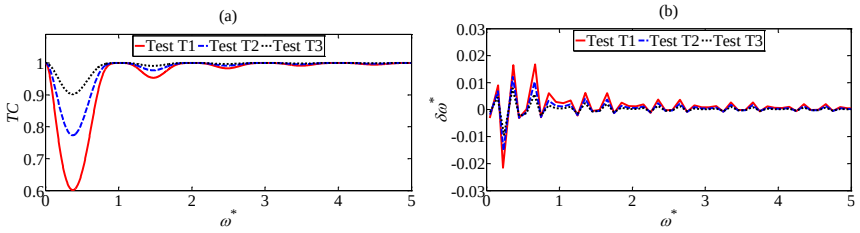

Figure 10. (a) Transmission coefficients of non-uniform unbounded blocked pipeline systems; (b) frequency shifts of bounded systems induced by non-uniform blockages

As shown in Table 2, the blockage severity of Tests T1, T4, and T5 is fixed. The length of the non-uniform blockages gradually decreases from 100 m to 1m. Similar TC curves (for unbounded system) and frequency shift patterns (for bounded system) can be observed in Figures 11(a) and 11(b), respectively. Moreover, both TC curves and frequency shift patterns of these three tests almost coincide with each other. This means that the non-uniform blockage length has little influence on the amount of energy transmitted through the non-uniform blockages.

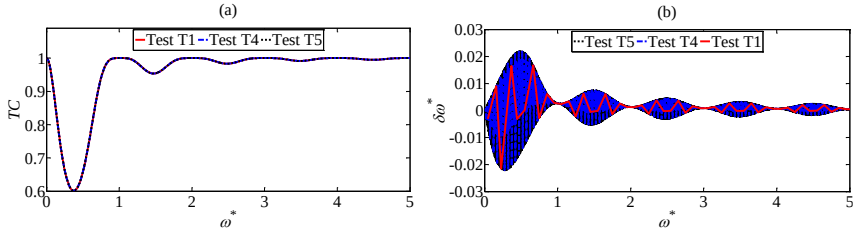

Figure 11. (a) Transmission coefficients of non-uniform unbounded blocked pipeline systems; (b) frequency shifts of bounded systems induced by non-uniform blockages

5 DISCUSSION OF RESULTS

In previous studies (14, 20), the amplitude of transmitted and reflected waves (equivalent to transmitted and reflected energy) of an unbounded pipeline system with a uniform blockage is calculated by applying the mass and momentum conservation at pipe junctions (i.e., sudden constriction and expansion). However, the pipe diameters of pipeline systems with non-uniform blockages change continuously along the axial direction. This means that the diameters of the intact and blocked sections are the same at pipe junctions. Thus, the previous method cannot be applied to pipeline systems with non-uniform blockages for TC calculations. Based on the system overall transfer matrix, this paper proposed a new approach that is suitable for estimating the energy transmitted through the non-uniform blockages. The derived result (i.e., Eq. (26)) can be also applied to pipeline systems containing multiple non-uniform blockages, which is more practical, once the system overall transfer matrix is determined.

The results and findings above demonstrate that the frequency shifts of bounded pipeline systems induced by non-uniform blockages become less evident as the increase of the incident wave frequency. This can be explained by the TC curves of unbounded pipeline systems that more energy is transmitted through the non-uniform blockages as the incident wave frequency increases. This means that non-uniform blockages have a less blocking effect on the propagation of relative high frequency incident waves. Therefore, the frequency shifts of pipeline systems containing non-uniform blockages become less evident for higher frequency incident waves.

In practical applications of non-uniform blockage detection, it is a preferable and labour-saving way to place the transient wave receiver at the same accessible point with the generator. Understanding the TC of incident waves in various frequencies provide valuable insights into the blocking effect of non-uniform blockages on transient waves. It is useful for the selection of incident wave frequency and bandwidth to ensure that the reflected waves have enough energy for the pressure transducer (i.e., receiver) to measure. Otherwise, the reflected waves, which have limited energy, may be buried by the background noises. In this case, the transient frequency shifts of this measured signal may be less evident that cannot be used to detect the non-uniform blockages accurately.

6 CONCLUSIONS

paper explains the frequency shift pattern induced by non-uniform blockages in pressurised water pipelines from an energy perspective. First, the overall transfer matrix of a pipeline system containing exponential non-uniform blockages is analytically

derived based on the 1D plane wave solutions. The overall transfer matrix is then used to derive the TC, which is numerically validated by the MOC. Finally, the frequency shift pattern of bounded pipeline systems with non-uniform blockages is explained by TC curves of unbounded pipeline systems.

The results indicate that the frequency shift pattern induced by exponential non-uniform blockages, which becomes less evident as the increase of the incident wave frequency, is similar with that induced by linear non-uniform blockages. The energy analysis shows that the higher the incident wave frequency, the more energy is transmitted through the non-uniform blockages. This means that the non-uniform blockages have a less blocking effect on the propagation of high frequency waves; thus, the induced frequency shifts become less evident.

In practical applications of non-uniform blockage detection, the frequency and bandwidth of the incident wave should be selected carefully according to the TC curve to ensure that the reflected wave contains enough energy.

7 ACKNOWLEDGEMENT

This work was supported by (1) the Hong Kong Research Grants Council (RGC) with projects 25200616, 15201017 and T21-602/15R; and (2) the Hong Kong Polytechnic University with projects 1-ZVGF and 3-RBAB.

8 REFERENCE

(1) Henry, R., and Luxmoore, A. R., 1996, "A pipe-profiling adapter for CCTV inspection cameras: Development of a pipe-profiling instrument," Measurement Science and Technology, 7(4), pp. 495-504.
(2) Brunone, B., and Ferrante, M., 2001, "Detecting leaks in pressurised pipes by means of transients," Journal of Hydraulic Research, 39(5), pp. 539-547.
(3) Lee, P. J., Lambert, M. F., Simpson, A. R., Vítkovský, J. P., and Liggett, J. A., 2006, "Experimental verification of the frequency response method for pipeline leak detection," Journal of Hydraulic Research, 44(5), pp. 693-707.
(4) Sattar, A. M., and Chaudhry, M. H., 2008, "Leak detection in pipelines by frequency response method," Journal of Hydraulic Research, 46(sup1), pp. 138-151.
(5) Colombo, A. F., Lee, P. J., and Karney, B. W., 2009, "A selective literature review of transient-based leak detection methods," Journal of Hydro-environment Research, 2(4), pp. 212-227.
(6) Duan, H. F., Lee, P. J., Ghidaoui, M. S., and Tung, Y. K., 2011, "Leak detection in complex series pipelines by using the system frequency response method," Journal of Hydraulic Research, 49(2), pp. 213-221.
(7) Lee, P. J., Vitkovsky, J. P., Lambert, M. F., Simpson, A. R., and Liggett, J. A., 2008, "Discrete blockage detection in pipelines using the frequency response diagram: Numerical study," Journal of Hydraulic Engineering, 134(5), pp. 658-663.
(8) Meniconi, S., Brunone, B., and Ferrante, M., 2010, "In-line pipe device checking by short-period analysis of transient tests," Journal of Hydraulic Engineering, 137(7), pp. 713-722.
(9) Sattar, A. M., Chaudhry, M. H., and Kassem, A. A., 2008, "Partial blockage detection in pipelines by frequency response method," Journal of Hydraulic Engineering, 134(1), pp. 76-89.

(10) Wang, X. J., Lambert, M. F., and Simpson, A. R., 2005, "Detection and location of a partial blockage in a pipeline using damping of fluid transients," Journal of Water Resources Planning and Management, 131(3), pp. 244-249.
(11) Duan, H. F., and Lee, P. J., 2015, "Transient-based frequency domain method for dead-end side branch detection in reservoir pipeline-valve systems," Journal of Hydraulic Engineering, 142(2), p. 04015042.
(12) Duan, H. F., Lee, P. J., Ghidaoui, M. S., and Tung, Y. K., 2012, "Extended blockage detection in pipelines by using the system frequency response analysis," Journal of Water Resources Planning and Management, 138(1), pp. 55-62.
(13) Duan, H. F., Lee, P. J., Kashima, A., Lu, J., Ghidaoui, M. S., and Tung, Y. K., 2013, "Extended blockage detection in pipes using the system frequency response: analytical analysis and experimental verification," Journal of Hydraulic Engineering, 139(7), pp. 763-771.
(14) Louati, M., Ghidaoui, M. S., Meniconi, S., and Brunone, B., 2018, "Bragg-type resonance in blocked pipe system and its effect on the eigenfrequency shift," Journal of Hydraulic Engineering, 144(1), p. 04017056.
(15) Duan, H. F., Lee, P. J., Che, T. C., Ghidaoui, M. S., Karney, B. W., and Kolyshkin, A. A., 2017, "The influence of non-uniform blockages on transient wave behavior and blockage detection in pressurized water pipelines," Journal of Hydro-environment Research, 17, pp. 1-7.
(16) Che, T. C., Duan, H. F., Lee, P. J., Pan, B., and Ghidaoui, M. S., 2018, "Transient frequency responses for pressurized water pipelines containing blockages with linearly varying diameters," Journal of Hydraulic Engineering.
(17) Che, T. C., Duan, H. F., Lee, P. J., and Ghidaoui, M. S., 2017, "Theoretical Analysis of the Influence of Blockage Irregularities on Transient Waves in Water Supply pipelines," The 37th IAHR World Congress, Kuala Lumpur, Malaysia, pp. 5800-5809.
(18) Chaudhry, M. H., 2014, Applied hydraulic transients, Springer-Verlag, New York.
(19) Blackstock, D. T., 2000, Fundamentals of physical acoustics, John Wiley & Sons.
(20) Duan, H. F., Lee, P. J., Ghidaoui, M. S., and Tuck, J., 2014, "Transient wave-blockage interaction and extended blockage detection in elastic water pipelines," Journal of fluids and structures, 46(2014), pp. 2-16.
(21) Munjal, M. L., 2014, Acoustics of ducts and mufflers, John Wiley & Sons.
(22) Joukowsky, N. E., 1898, "Memoirs of the Imperial Academy Society of St. Petersburg," Proceedings of the American Water Works Association, 24, pp. 341-424.